ON THE AUGMENTATION OF LOWER BOUND PLASTIC LIMIT LOADS OF IMPERFECT STRUCTURES DUE TO STRESS AND STRAIN HARDENING

H.-J. Golembiewski*, G. Vasoukis*

The failure of flawed structures is governed by a critical net section stress if the material's ductility is adequate. This work deals with two effects that may raise actual failure loads above the theoretical lower bound estimate, namely the plastic hardening due to increasing plastic strain and the plastic hardening due to reorientation of stress components within the plastic regions. An evaluation of 1200 fracture mechanics experiments on a huge variety of specimen and component geometries made of various steels commonly used for nuclear power plant components has been performed. The ratio of yield stress to ultimate tensile strength R_p/R_m serves as the index of the material's strain hardening capacity.

INTRODUCTION

The safety assessment of nuclear pressure retaining components with anticipated or actual flaws is effectually achieved by the net section collapse method. The very ductile materials, of which these components are made, generally provide assurance at all temperatures of operation that a certain load calculated by plastic limit load formulae is endured without failure.

An evaluation of 1200 fracture mechanics experiments on a multitude of geometries has indicated that a minimum Charpy absorbed energy of 45 J is required, provided that the strain hardening of the material and the multiaxiality of stress state are not considered, see Fig. 1, Golembiewski and Vasoukis (1).

In the following paragraphs we relate the experimental maximum load of these tests to the thus-calculated theoretical limit load to determine the effect of material strain hardening and of stress state on the failure load.

An evaluation split up into specimen shapes, specimen sizes, crack sizes and materials has been performed in some instances but

* Siemens AG, UB KWU, Erlangen, FRG

for the sake of conciseness this has not been included in the present paper.

STRAIN HARDENING

Just how much a material can raise its elastic stress limit with increasing plastic strain is clearly obvious in any uniaxial tensile test. With ductile fracture concepts this material capacity is generally accounted for by the use of a flow stress, e. g. the mean of yield and ultimate tensile strength. However, many series of fracture mechanics tests reveal that such a flow stress renders limit load predictions nonconservative, see Rosezin (2) or Dahl and Zeislmair (3). Indeed, the net section of these structures has completely plastified, hence plastic limit load has been attained. With integrity assessments of flawed structures, ideally plastic material behaviour, as is always assumed in elementary plasticity theory, ascertains that critical crack dimensions or maximum load predictions lie on the safe side.

An index of a material's strain hardening capacity is given by the ratio of yield stress to ultimate tensile strength R_p/R_m, although this ratio does not reflect the amount of plastic strain involved. The comparison of the experimental maximum load (P_{max}) with the lower bound plastic limit load (P_L) calculated without strain hardening indicates (Fig. 2) that this load can be attained ($P_{max}/P_L \geq 1$) at all values of stress ratio considered (R_p/R_m= 0.3 - 0.9). Tests that did not arrive at P_{max}/P_L= 1 were performed on materials keeping ratios R_p/R_m generally greater than 0.67. In this figure the circles and crosses differentiate between materials of, respectively, greater and less than 45 J Charpy absorbed energy. The results which lie significantly below the line P_{max}/P_L = 1 are those from tests on materials of less than 45 J, reference (1).

Figures 3a and 3b depict the results of experiments in a plane of material properties, the stress ratio R_p/R_m on the abscissa and Charpy absorbed energy C_v on the ordinate. Here single points may represent series of tests; Figure 3a covers the results of all experiments. The circles and crosses stand for experiments with ratios P_{max}/P_L greater and smaller than 1, respectively.

If one concentrates on the experiments that failed to reach the theoretical lower bound limit load, viz. the crosses in Figure 3b, the regime of non-attainment becomes obvious: A rather sharp delineation in terms of absorbed energy at 45 J and, in terms of stress ratio R_p/R_m, an accumulation above 0.67.

Finite element analyses have been performed to demonstrate the real benefit of strain hardening to the plastic limit load. A 75 mm thick compact tension specimen undergoing mainly bend type loading was modelled three-dimensionally around the crack

tip and across the ligament and two-dimensionally (plane stress) at other places, see Fig. 4. Additionally, a simple two-dimensional mesh of indentical elements was used to obtain plane stress and plane strain results. The crack length to width ratio a/W was 0.6. In each numerical calculation the load was increased until the plastic zone had closed across the ligament. This load is considered the numerical plastic limit load. Figure 4 shows the load versus crack opening displacement at load line for all the simulations performed. The two- and three-dimensional idealizations were performed once assuming ideally plastic material behaviour (yield stress R_p = 428 MPa) and then again assuming a multilinear approximation of the strain hardening properties of the material (R_p/R_m = 0.68). The three-dimensional calculation including strain hardening is thought to be the most realistic simulation and indeed is verified by four experiments to an accuracy of better than 1 % in load and displacement. By comparing the two calculations of the three-dimensional type in Figure 4 one realizes that strain hardening augments the plastic limit load by some 5 % with this geometry. The plastic limit load formula given by Merkle and Corten (4) and Kumar et al. (5) applied with a flow stress as the mean of yield and ultimate tensile strength will in this case result in an apparent 23 % augmentation due to strain hardening.

STRESS HARDENING

In contrast to strain hardening, which is a material characteristic, the so-called stress hardening must be attributed to the geometry of the structure. Within plastically deforming regions this process is controlled by the reorientation of stress components in the course of increasing load. A higher stress triaxiality ensues and hinders the plastic region from spreading. The phenomenon is expected to appear preferentially with geometries which promote multiaxiality of the stress state such as specimens and components containing notches or cracks.

Limit load relations given in references (4) and (5) for compact tension specimens reveal to what degree the load carrying capacity of a cracked structure is augmented theoretically by such a hindrance of plastic flow: the plastic limit load in plane strain state surpasses the limit load in plane stress by 36 % and the uniaxial limit load by 45 %. On the other hand finite element results support the concept of the multiaxial stress state being contained to a small volume around the crack tip. Further away from the tip only two-dimensional stress states prevail and dominate the global behaviour of the structure. Following this reasoning higher load carrying capacities for bigger specimens, sharper or deeper cracks or notches connot be expected in the amount predicted by plasticity theory. On the contrary, the gain in load carrying capacity of larger specimens due to stress hardening (higher triaxiality of the stress state) appears to be overtaken by the loss in load carrying capacity due to less plastic

deformation, hence less strain hardening.

This is demonstrated in Fig. 5 by experiments on compact tension specimens of various sizes (standard CT-specimens, thickness B) made of the same ductile material: the larger the specimen, the less the relative maximum load P_{max}/P_L. The tendency is expressed by a linear regression on all data points. This tendency is common to all specimen and component geometries if the length of the crack front is considered the measure of the structure's size. Furthermore the theoretical plastic limit load of plane strain state given in reference (5) is not attained by the large specimens although the yield stress has been used to calculate P_L (Fig. 5). The tendency is found to be more pronounced, the greater the bending part of the loading on the flawed section. Specimens loaded only in tension often do not show this behaviour. Even greater relative maximum load with larger specimen sizes has been observed on purely tensile fracture specimens, Roos (6).

However, the general loading on the section of a structure will include bending, which obviously lessens the ratio P_{max}/P_L upon increasing section size. Therefore in safety assessment it is prudent and realistic to apply plastic limit load formulae only in plane stress state. By doing this, the ductile failure load of flawed structures of specimens of whatever size is estimated on the safe side.

CONCLUSIONS

The two distinct phenomena - material strain hardening and geometrical stress hardening - do not contribute to the augmentation of a structure's plastic limit load in the amount advocated by general opinion and elementary plasticity theory. To detail the share of each phenomenon for a given structure and material, one has to analyze the elastic-plastic strain field and calculate the corresponding stress field. So far elaborate numerical methods are required to solve these problems. Alternatively a simple procedure given in reference (1) to estimate a lower-bound plastic limit load relies obligatorily on the use of the yield stress and the plane stress state. This method yields limit loads which a flawed structure will safely bear provided the material is of adequate ductility ($C_v > 45$ J).

REFERENCES

(1) Golembiewski, H.-J. and Vasoukis, G., Int. J. Pres. Ves. and Piping 24, 1986, p. 27 - 36

(2) Rosezin, H.-J., "Beurteilung des Bruchverhaltens von Stählen auf der Grundlage von Großzugversuchen", Dissertation, 1983, Rheinisch-Westfälische Technische Hochschule, Aachen, FRG

(3) Dahl, W. and Zeislmair, H.-C., "Anwendung der Bruchmechanik auf Baustähle", Verlag Stahleisen mbH, Düsseldorf, 1983, FRG

(4) Merkle, J. G. and Corten, H. T., ASME J. Pres. Ves. Technol., 1974, pp. 1 - 7

(5) Kumar, V., German, M. D., Shih, C. F., EPRI, NP - 1931/ RP 1237-1, 1981, Palo Alto, California, USA

(6) Roos, E., "Grundlagen, Anwendungsmöglichkeiten und Anwendungsgrenzen der Zähbruchkonzepte", 17. Technischer Bericht, Schriftenreihe Reaktorsicherheit Bundesminister für Umwelt, Natur- und Strahlenschutz und Reaktorsicherheit, BMU-1986-112, Sept. 1986, Bild 55, Bonn, FRG

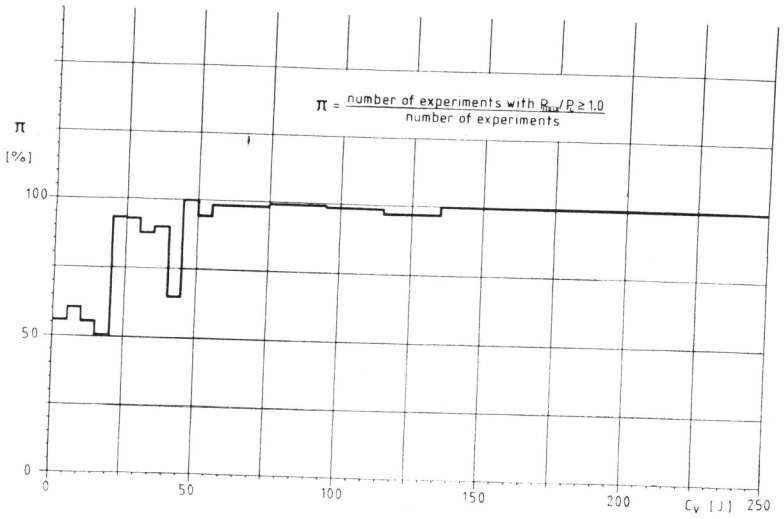

Figure 1 Percentage of attainment (π) of the lower bound limit load within Charpy absorbed energy (C_V) intervals

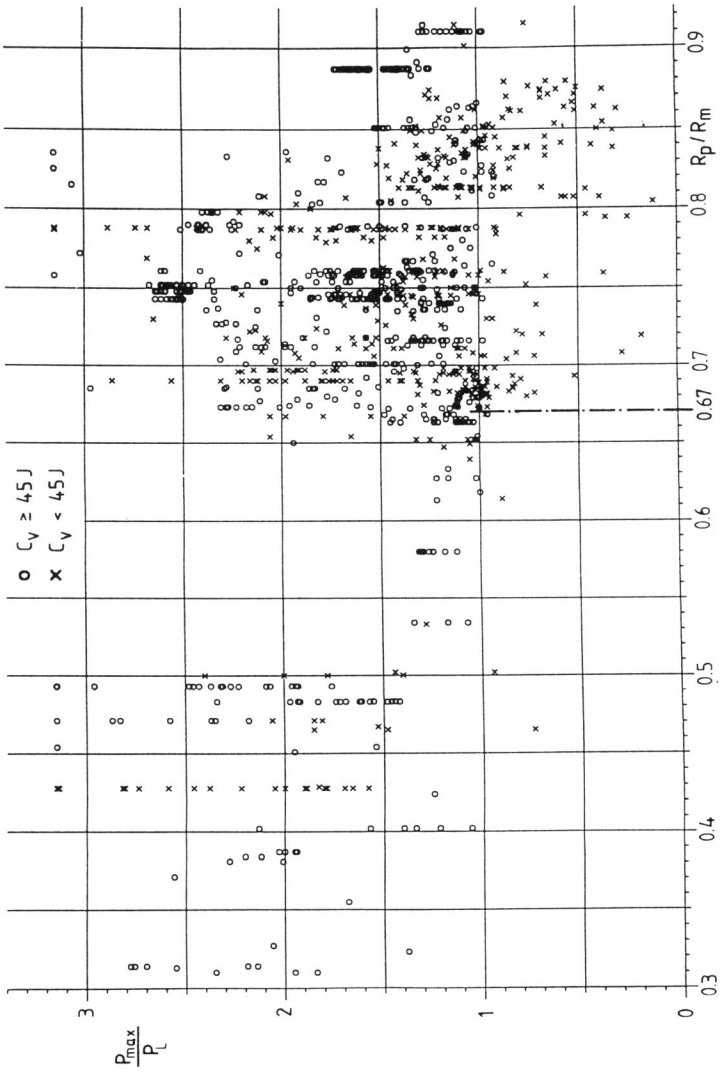

Figure 2 Ratio of maximum load P_{max} to lower bound limit load P_L related to the material's yield stress to ultimate tensile strength ratio R_p/R_m

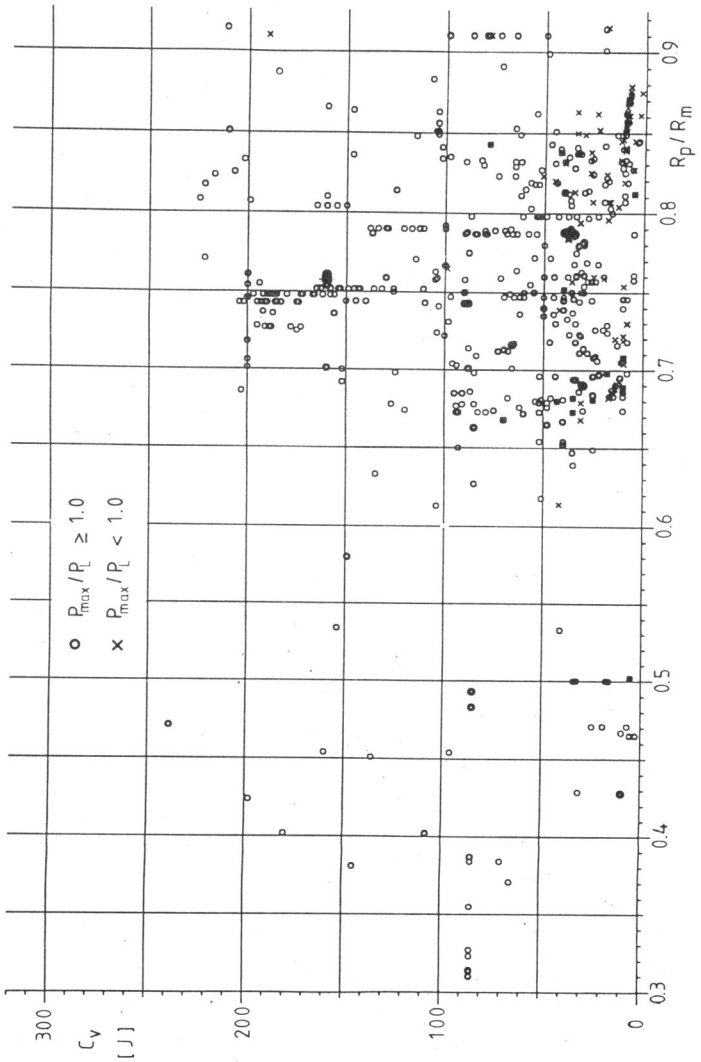

Figure 3a Material properties Charpy absorbed energy C_v and yield stress to ultimate tensile strength ratio R_p/R_m of all tests evaluated

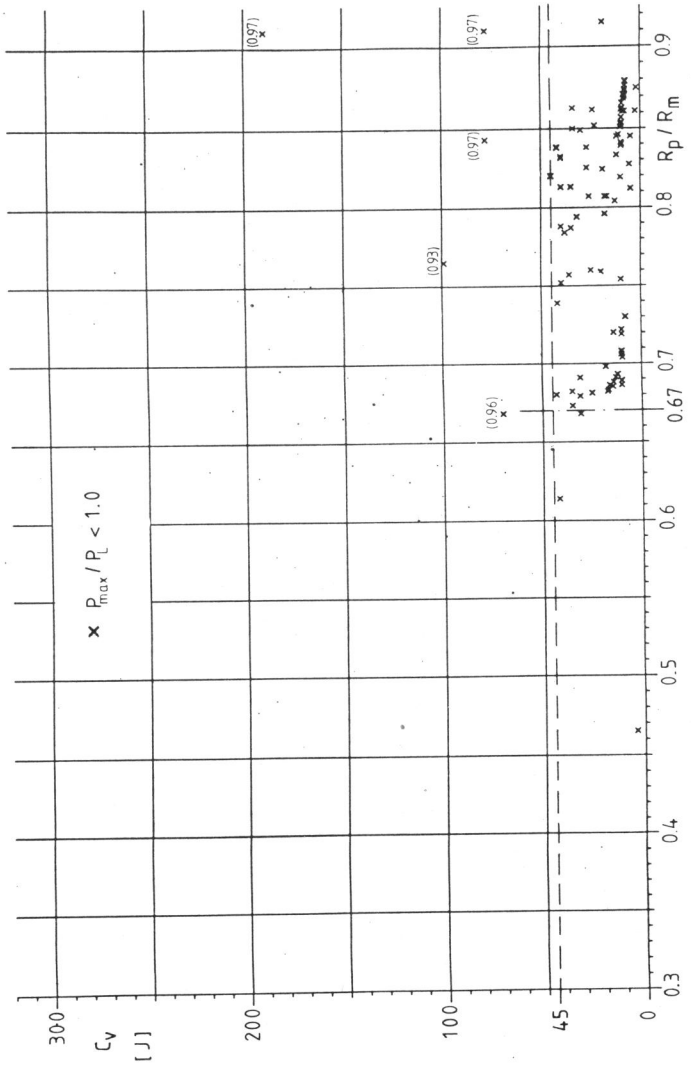

Figure 3b As Figure 3a but only tests that did not reach the lower bound limit load

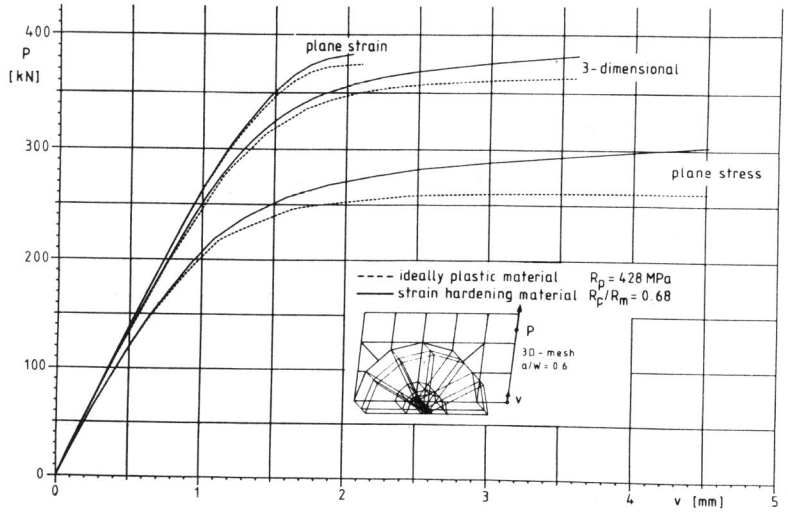

Figure 4 Load versus displacement of a 75 mm-standard compact specimen up to net section yield, finite element results

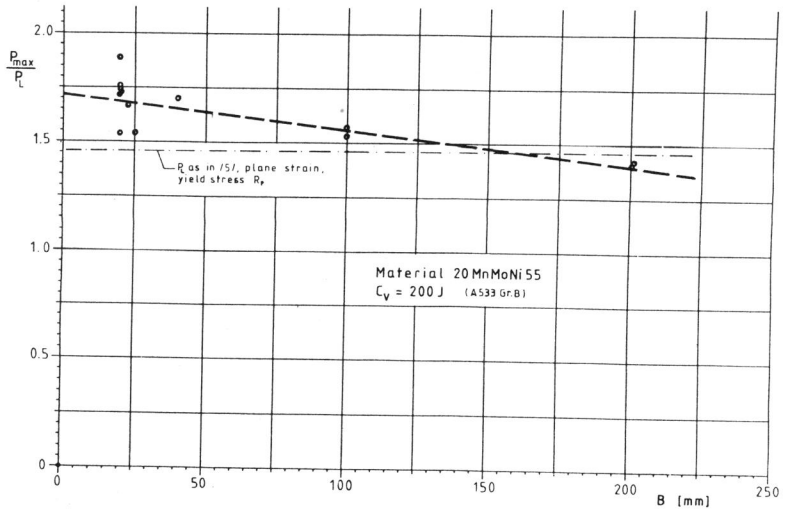

Figure 5 Test results of standard compact specimens (fatigue precracked) of varying size (represented by specimen thickness B) but of the same material (results of German Reactor Component Safety Research Program)